



## Spectroscopy of super heavy elements with GABRIELA

A. Lopez-Martens, K. Hauschild

### ► To cite this version:

A. Lopez-Martens, K. Hauschild. Spectroscopy of super heavy elements with GABRIELA. The European physical journal. A, Hadrons and Nuclei, 2022, 58 (7), pp.134. <10.1140/epja/s10050-022-00787-7>. <hal-03758475>

**HAL Id: hal-03758475**

**<https://hal.science/hal-03758475v1>**

Submitted on 7 Nov 2022

**HAL** is a multi-disciplinary open access archive for the deposit and dissemination of scientific research documents, whether they are published or not. The documents may come from teaching and research institutions in France or abroad, or from public or private research centers.

L'archive ouverte pluridisciplinaire **HAL**, est destinée au dépôt et à la diffusion de documents scientifiques de niveau recherche, publiés ou non, émanant des établissements d'enseignement et de recherche français ou étrangers, des laboratoires publics ou privés.



HAL Authorization

# Spectroscopy of super heavy elements with GABRIELA

A. Lopez-Martens · K. Hauschild · and  
the GABRIELA collaboration

Received: date / Accepted: date

**Abstract** The spectrum of states in very heavy and super heavy nuclei is the result of a delicate balance between the strong Coulomb repulsion between the numerous protons in the nucleus and the properties of the strong force acting between the many nucleons in the system. Fine-structure  $\alpha$  decay combined with  $\gamma$ -ray and internal-electron-conversion spectroscopy allows to identify the sequence and energies of low-lying nuclear states. This information can then be used to constrain the parameters that define the nuclear mean-field and thus improve the reliability of predictions in a region controlled critically by small shell effects. Detailed spectroscopy of transfermium nuclei is the prime motivation of the Franco-Russian GABRIELA (Gamma Alpha Beta Recoil Investigation with the ELectromagnetic Analyzer) project, launched more than 15 years ago. The current review aims at presenting the experimental developments that have been carried out over the years and discuss a selection of results that have been obtained.

**Keywords** Heavy elements · Super heavy elements · Decay spectroscopy · Nuclear structure · Fission

## 1 Introduction

One of the major challenges of modern Nuclear Physics is to investigate the limits of nuclear existence. A simple and yet fundamental question is: what is the maximum number of protons and neutrons a nucleus can sustain? To answer such a question, the synthesis of new elements with an ever increasing

---

A. Lopez-Martens  
Université Paris Saclay, IJCLab CNRS-IN2P3  
Tel.: +33 1 69 15 48 50  
E-mail: araceli.lopez-martens@ijclab.in2p3.fr

K. Hauschild  
Université Paris Saclay, IJCLab CNRS-IN2P3

number of protons is carried out and motivated by the theoretical prediction of a new island of stability. Super heavy nuclei also provide a unique laboratory within which nuclear structure and dynamics under very intense Coulomb forces can be studied. While cross-sections to synthesize the heaviest elements are extremely low, the production rate of super heavy nuclei with proton numbers ranging from  $Z=100$  to  $Z=106$  is high enough to obtain significant information on their nuclear structure via spectroscopic studies.

Spectroscopic studies beyond Es ( $Z=99$ ) have made great progress in recent years due to the use of efficient detector arrays around the target position (prompt spectroscopy) and at the focal plane of recoil separators (decay spectroscopy). These have revealed that super heavy nuclei are very robust with respect to rotation, reaching spins of more than  $20 \hbar$  and revealing interesting alignment properties [1]. Some of the most hindered decays in the whole of the nuclear chart have been observed from high- $K$  isomers in the region around  $^{254}\text{No}$  [2]. Fine structure  $\alpha$  decay has allowed trends in low-energy structures to be established as a function of  $N$  and  $Z$ . From this body of data, there exists now a rather clear disagreement between the predictions of single-particle sequences and shell gaps obtained from all existing effective interactions/energy density functionals and experiment. The data, however, remain scarce and clustered to nuclei reached by fusion evaporation reactions with Pb and Bi targets with large cross sections or transfer reactions on long-lived actinide targets.

Decay spectroscopy of heavy elements is carried out only in a few places around the world: at Argonne National Laboratory (USA), in GANIL (France), at GSI (Germany), at the FLNR Dubna laboratory (Russia), at JAEA (Japan), in Lanzhou (China), at the Lawrence Berkeley National Laboratory (USA) and at the University of Jyväskylä (Finland). Each facility has its specificities (especially in terms of beam characteristics, availability of targets, recoil separation techniques, detection setups and available spectroscopic observables) but there is of course some overlap and the competition is strong. This is a healthy situation as it forces the physicists and engineers to improve their experimental setup in every way they can. Moreover, it is a guarantee that results are cross-checked, which is essential in this field of very rare events.

The project of  $\alpha$ ,  $\gamma$ , X-ray and internal-conversion electron (ICE) spectroscopy studies at the FLNR was launched by an IN2P3-JINR collaboration in 2003. Since then, it has been in constant evolution. In this review, the major steps of this evolution will be presented. The next section is devoted to present a selection of results on properties of super heavy nuclei in the region around  $^{254}\text{No}$ , with special emphasis on internal-conversion spectroscopy results. The last section will be devoted to describe perspectives and future plans.

## 2 The GABRIELA array

### 2.1 GABRIELA at VASSILISSA

The Gamma Alpha Beta Recoil Investigations with the ELeCtromagetic Analyzer (GABRIELA) detector array was designed and built in 2004. As illustrated in Fig. 1, it was installed at the focal plane of the VASSILISSA separator [3], where it is shielded from the principal components of the separator, the target and the beam dump by a 2 m concrete wall. Additional background suppression of scattered beam particles is provided by a deflector magnet installed behind the separator.

The setup consisted of a Time-of-Flight (TOF) detector and a 16-resistive-

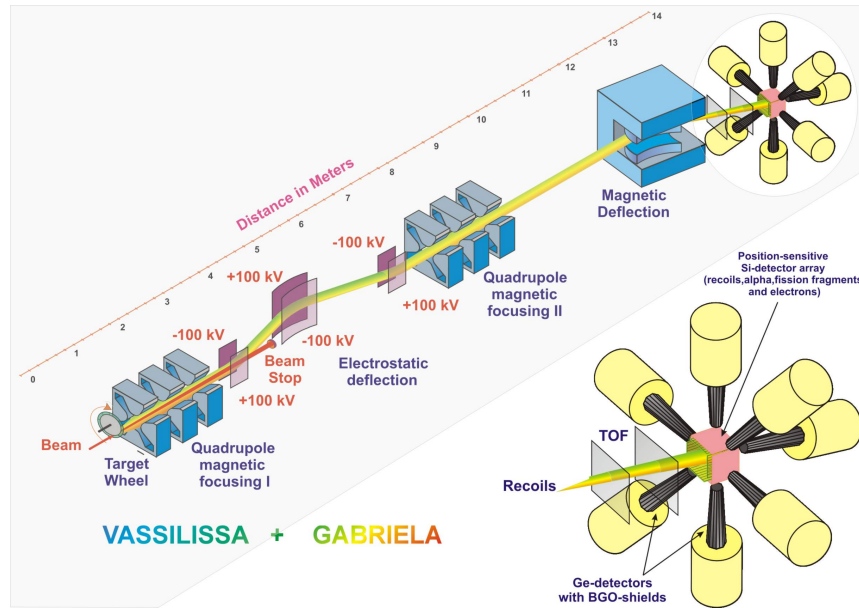


**Fig. 1** Schematic illustration of the VASSILISSA separator and of the GABRIELA detector array.

strip Si detector for implanting the recoiling nuclei produced at the target and detecting their subsequent charged particle emission ( $\alpha$  or fission). In the backward direction, four 4-fold segmented Si detectors forming a tunnel were used to detect the escaping particles ( $\alpha$  particles, fission fragments and ICES). All around the Si detectors, seven HPGe detectors from the France-UK Loan Pool were placed in a compact configuration to detect photons and X rays. The performance in terms of  $\gamma$ -ray and ICE resolutions and efficiencies of this first setup are given in [4]. The background rate in the Ge detectors of the GABRIELA array was further reduced by surrounding them with anti-Compton BGO shields, also from the France-UK Loan Pool. This resulted in

a typical global GABRIELA count rate of a few hundred Hz with beam on target. Despite the high thresholds of the implantation detector, which was therefore only sensitive to  $\alpha$  decay and fission, the background rejection of VASSILISSA allowed to observe correlations between an implantation signal in the DSSD and an isomer-decay signal in the tunnel detectors, as will be discussed in Sect. 3.

To increase the efficiency of the  $\gamma$ -ray detection array, a modification to the Ge detector placed behind the implantation detector was made in 2006. The distance between the Ge crystal and the front face of the detector aluminium end cap was reduced to a few mm. This resulted in a increase of the overall  $\gamma$ -ray efficiency by a factor of 2. A further modification to the setup was made in 2009 by replacing the resistive strip implantation detector by a similar-sized Double-sided Silicon Strip Detector (DSSD) manufactured by RIMST (Zelenograd, Russia). It had 48 vertical and 48 horizontal strips and was instrumented with 3 different amplification ranges, allowing to detect signals as low as 100 keV,  $\alpha$  particles up to 20 MeV as well as 200 MeV fission signals [5]. This opened the field of research at GABRIELA to the study of long-lived isomers using Jones' isomer-decay tagging technique [6]. This technique relies on the detection of a low-energy pulse, which arises when the isomeric decay proceeds through a cascade of highly-converted transitions. The tunnel detectors were also replaced by 32-fold segmented Si detectors to improve the energy resolution for ICE spectroscopy.

## 2.2 GABRIELA at SHELS

In the first years of the GABRIELA project, the experiments suffered from the poor transmission of the VASSILISSA separator. Funds were obtained in 2006 to upgrade and transform it into a velocity filter. The Separator for Heavy Element Studies (SHELS) was commissioned in 2013-2014 using a new large area 128x128 DSSD from MICRON SEMICONDUCTOR. A five-fold increase in the transmission of evaporation residues (ER) produced in asymmetric reactions with light beams was measured [7].

In a second round of funding, the focal plane detection system, which had been upgraded in 2006 and 2009, was vastly improved. State of the art Ge detectors were bought from MIRION increasing the photon detection efficiency by almost a factor of two. Dedicated BGO shields, designed within the collaboration, were also bought from SCIONIX. A new vacuum chamber was also built specifically for the revised GABRIELA detection system, with special thin aluminium inserts to position the Ge detectors as close as possible to the source of radiation and to maximise detection efficiency for low energy photons. The tunnel detection system was also upgraded and consists of eight 16x16 DSSD (see Fig. 2). The performance of the upgraded GABRIELA detection system are resumed in [8].

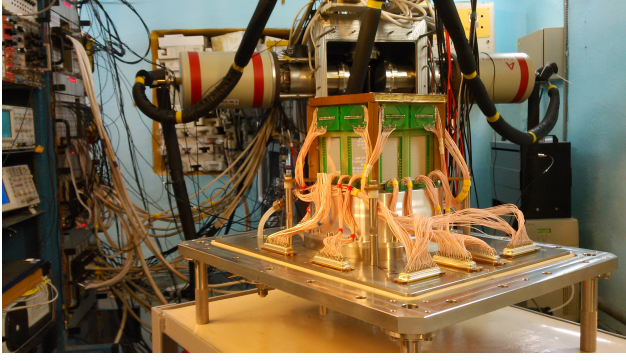


**Fig. 2** Photograph showing the back flange of the vacuum chamber revealing 2 faces of the tunnel detector in the foreground and the inside of the chamber with the special thin-window inserts for the  $\gamma$ -ray Ge detectors.

### 2.3 GABRIELA response function

The probability of ICE emission relative to  $\gamma$  emission increases with the atomic number  $Z$  of the nucleus and decreases rapidly with increasing transition energy. In heavy- $Z$  nuclei, internal conversion is therefore an important process. In the case of multiple coincident emissions, the internal conversion and the accompanying atomic relaxation processes may lead to important summing effects in the implantation DSSD. Pileup of photons will also occur in the different detectors of the Ge array. In order to understand, and properly interpret the observed energy spectra, Monte Carlo simulations with the GEANT4 package [9] (or equivalent) have become an important part of the data analysis. Such simulations were first done in the case of the  $\alpha$  decay of  $^{253}\text{No}$  to excited states in  $^{249}\text{Fm}$  studied at GABRIELA [10]. These were made possible in such heavy elements by hard-coding the list of primary particles corresponding to the radioactive emission sequences and the associated atomic relaxation processes of the nuclei of interest. More recently, modifications of various GEANT4 classes were made so that the simulation package may handle all the aspects of radioactive decays of elements beyond Fm [8].

On top of a precise implementation of the detector materials, geometries, relative positions and active volumes, a critical ingredient of the simulations is the average implantation depth of ERs in the DSSD. A novel technique was devised to estimate this depth by a  $\chi^2$  comparison between the experimental energy distribution of  $\alpha$  particles that escape from the DSSD and simulated distributions obtained using different implantation gaussian depth profiles [8]. The sensitivity of the method is illustrated in Fig. 3 for the case of the  $\alpha$  decay of  $^{215}\text{Ra}$  produced in the reaction  $^{198}\text{Pt}(^{22}\text{Ne}, 5n)$ .

Another aspect of the GABRIELA response function that was investigated was the efficiency of a  $\gamma$ -ray software trigger to identify spontaneous-fission events in the case where the chosen amplification range of the DSSD does not go beyond 20 MeV and fission signals appear as ADC overflows. In a series

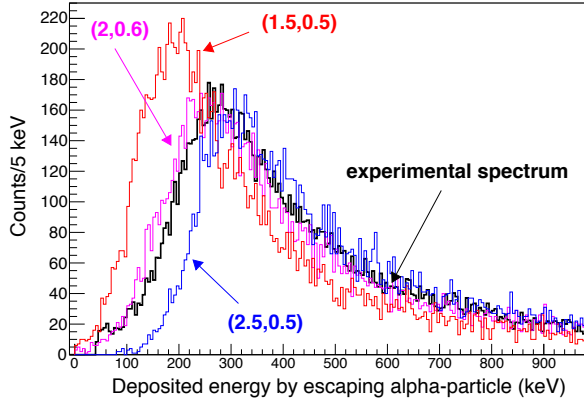


**Fig. 3** Experimental spectrum of deposited energies by escaping  $\alpha$  particles emitted by  $^{215}\text{Ra}$  (black) compared to simulated deposited energies for various gaussian implantation profiles of  $^{215}\text{Ra}$  nuclei. The average implantation depth  $d$  and standard deviation  $\sigma$  used in the simulations are given in brackets:  $(d, \sigma)$  in  $\mu\text{m}$ .

of experiments aimed at studying neutron-deficient No isotopes, GABRIELA was instrumented with different amplification ranges on the front and back strips of the DSSD (up to 20 MeV on the front and 200 MeV on the back). Fig. 4 shows the time distribution of detected front-strip ADC overflows with the condition that at least one  $\gamma$  ray be detected in coincidence in the reaction  $^{206}\text{Pb}(^{48}\text{Ca}, 2n)^{252}\text{No}$ . The comparison to the time distributions of back-strip decay events with energies larger than 30 MeV provides a measure of the efficiency of the  $\gamma$ -ray tag, which is found to reach  $\sim 93\%$  in this particular case. Using an *OR* of the tunnel and Ge-detector signals increases the fission tagging efficiency up to 97%.

### 3 Spectroscopy Results

#### 3.1 Systematics of low-lying excited states

The spectrum of excited states in super heavy nuclei is the result of a delicate balance between the strong Coulomb repulsion between the numerous protons in the nucleus and the properties of the strong force acting between the many nucleons in the system. Following the behaviour of states across isotonic chains allows to highlight how the system rearranges itself as neutrons or protons are added to the system and can reveal effects such as changes in the underlying single-particle spectra and the development of correlations.

The GABRIELA collaboration has focussed on studying the evolution of specific states in odd-N Fm, No and Rf isotopes; the  $5/2^+[622]$  and  $11/2^- [725]$  Nilsson states, highlighted in Fig. 5. These states lie below and above the  $N=152$  shell gap respectively. The  $5/2^+[622]$  state stems from the  $g_{9/2}$  shell,

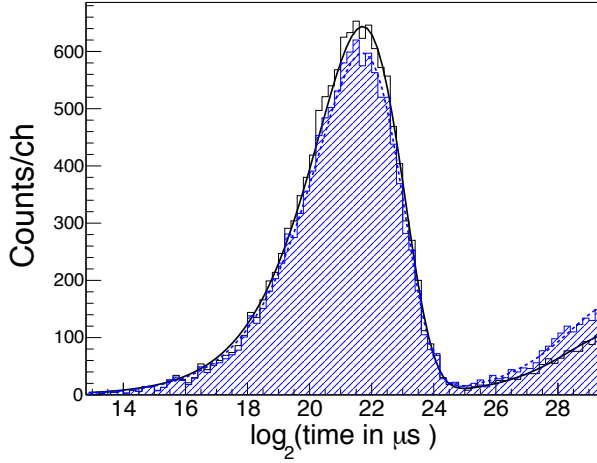


**Fig. 4** Time distribution (in binary logarithm of  $\mu\text{s}$ ) of decay events with measured energies greater than 30 MeV (black histogram) compared to the time distribution of ADC overflows detected in coincidence with at least one  $\gamma$  ray (blue hashed histogram). The solid and dashed lines represent 2-component fits to the distributions and yield 2.38(2) s for the ground-state activity of  $^{252}\text{No}$ , in agreement with the evaluated value [11].

while the  $11/2^- [725]$  state is an upsloping orbital as a function of axial deformation and originates from the  $j_{15/2}$  shell, as does the  $9/2^- [734]$  state lying just below the  $N=152$  gap. The position of the  $j_{15/2}$  shell at sphericity determines the size of the deformed  $N=152$  gap. It is also worth pointing out that the two above-mentioned shells differ by  $\Delta j = \Delta l = 3$ , which leads to octupole collectivity, as first investigated by Yates et al. [12] and addressed in the quasiparticle-phonon model by the Dubna group [13, 14].

### 3.1.1 $N=149$ isotones

Information on the low-lying structure of  $N=149$  isotones has mostly been obtained by fine structure  $\alpha$  spectroscopy of  $N=151$  nuclei, which are expected to have a ground state configuration based on the  $9/2^- [734]$  Nilsson configuration. This is comforted by the observed sequence of ground-state rotational states as well as their electromagnetic decay properties. Moreover, a nuclear spin of  $9/2 \hbar$  has recently been extracted from the splitting of the hyperfine structure of  $^{253}\text{No}$  [15], corroborating this picture.

The  $\alpha$  decay pattern of  $N=151$  isotones consists of a main branch to the  $9/2^- [734]$  state in the daughter nucleus, which then decays by E1 transitions to the  $7/2^+$ ,  $9/2^+$  and  $11/2^+$  members of the ground state rotational band. A small  $\alpha$ -decay branch also populates the  $5/2^+ [622]$  state, which decays to the ground state by an M1 transition.

In  $^{249}\text{Fm}$ , the M1 decay of the  $5/2^+$  state was first identified by  $\alpha$ -ICE spectroscopy using GABRIELA coupled to the VASSILISSA separator [10]. This



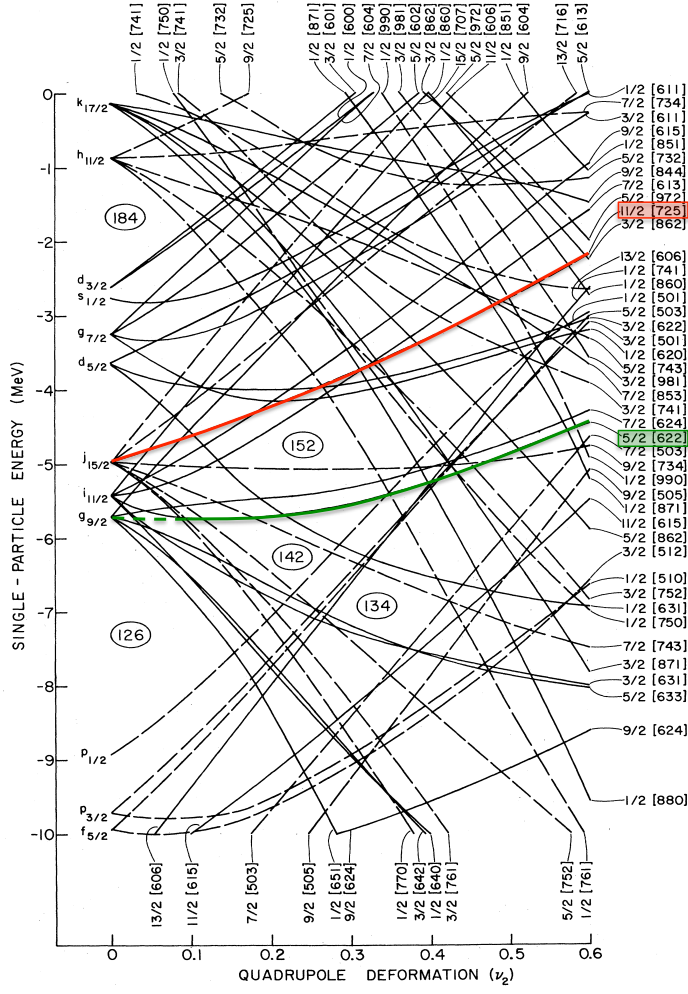


**Fig. 5** Nilsson diagram of neutron single-particle energies calculated with a Woods Saxon potential (adapted from Chasman et al., [18]). The orbitals discussed in the text ( $5/2^+ [522]$  and  $11/2^- [725]$ ) have been highlighted in green and red respectively.

finding was later confirmed by the observation of the corresponding weak  $\gamma$  ray emission at 209 keV at the focal plane of SHIP [16]. In the GABRIELA experiment, the internal-conversion coefficients of the E1 transitions stemming from the excited  $9/2^- [734]$  state were also measured. In the case of the 280 keV  $9/2^- \rightarrow 7/2^+$  transition, the  $K$  and  $LMN+$  conversion coefficients were found to be much higher than expected from theory [17], as also reported in the case of the lighter isotones  $^{245}\text{Cm}$  [18] and  $^{247}\text{Cf}$  [19]. In  $^{251}\text{No}$ , studied recently via the  $\alpha$  decay of  $^{255}\text{Rf}$  with GABRIELA at the

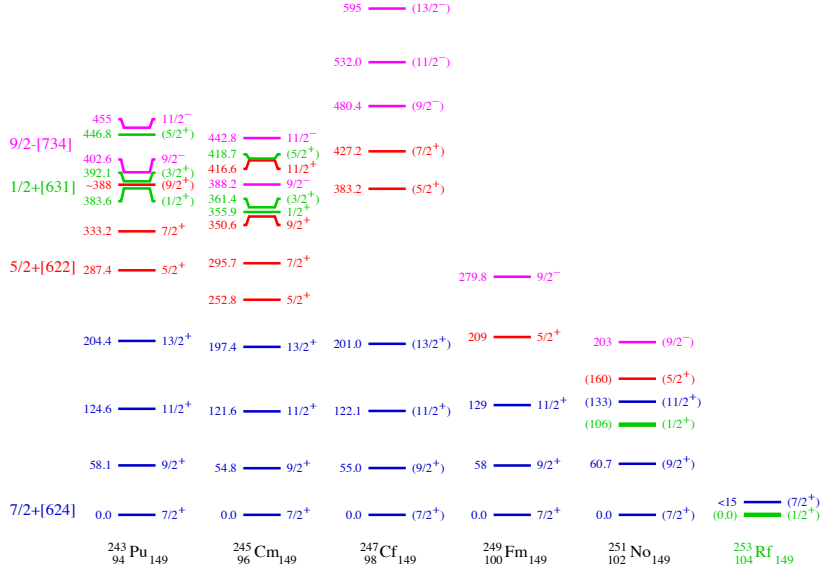


**Fig. 6** Systematics of the lowest states in N=149 isotones (data taken from Refs. [11, 23]).

focal plane of SHELS, only the  $LMN+$  conversion coefficient of the previously identified  $9/2^- \rightarrow 7/2^+$  203 keV transition [20] could be extracted from the combined  $\gamma$ -ray and ICE information. As before, the measured value was found to be anomalous [21]. Such anomalous E1 internal coefficients are not uncommon in the heavy mass region (see appendix D in Ref. [18]) and are thought to arise due to the combination of penetration effects and retardation of the  $\gamma$ -decay rate. Regarding the M1 decay of the  $5/2^+[622]$  state, the contribution of a low-energy M1 transition could not be unambiguously disentangled from the observed  $\alpha$ -ICE correlations due to the  $9/2^- \rightarrow 9/2^+$  143 keV transition, however, an excess strength at electron energies  $\sim 130$  keV was observed, which might suggest that the  $5/2^+[622]$  state lies at an excitation energy of  $\sim 160$  (i.e just above the  $K$  binding energy of No). The experiment also revealed a new  $\gamma$ -ray transition of  $\sim 70$  keV possibly depopulating the  $9/2^- [734]$  state and feeding the  $11/2^+$  member of the ground state band. The  $11/2^+$  state would then have an excitation energy of 133 keV. Regarding the last-known N=149 isotone, recent experimental data has confirmed the existence of two fissioning states in  $^{253}\text{Rf}$  [22, 23], most likely based on the  $7/2^+[624]$  and  $1/2^+[631]$  neutron configurations. The lower-spin state is also observed to have a 17(6)%  $\alpha$ -decay branch to the newly-discovered isotope  $^{249}\text{No}$  [22, 24, 25]. The ordering of the states in  $^{253}\text{Rf}$  could not be determined, but based on the known decoupling parameter of the  $1/2^+[631]$  band in lighter nuclei, a maximal excitation energy of  $\approx 15$  keV could be given to the  $7/2^+[624]$  state.



population in the  $\alpha$  decay of N=153 isotones, whose ground state is assigned the  $1/2^+$ [620] Nilsson configuration up to  $^{257}\text{Rf}$  (see Fig. 8). Using the early implementation of GABRIELA at VASSILISSA and looking at delayed correlations between signals in the tunnel and Ge detectors and the implantation signal from ERs in the DSSD, it was shown that the  $5/2^+$  isomer in  $^{253}\text{No}$ , first observed by Bemis et al. [27], decays by the emission of a 167 keV M2 transition [28]. This resolved the discrepancy between the observation of isomeric  $K$  Xrays by Bemis and the below-K-binding excitation energy of the  $5/2^+$ [622] state deduced from fine structure  $\alpha$ -decay spectroscopy of  $^{257}\text{Rf}$  [29].

The E3(M2) nature of the 200 keV  $5/2^+ \rightarrow 9/2^-$  transition in  $^{251}\text{Fm}$  had been determined from the ratio of the intensity of isomeric K X rays and the intensity of the 200 keV  $\gamma$  ray at GSI [20]. Combining  $\alpha$ - $\gamma$  and  $\alpha$ -ICE data taken with GABRIELA at SHELS and VASSILISSA and using a new graphical technique [30], the E3(M2) mixing ratio of the 200 keV transition was measured to be  $\delta=0.76_{-0.19}^{+0.20}$  [31]. Together with the measurement of the isomer lifetime, this in turn allowed to extract a value of 17.9(60) W.u for the B(E3) strength out of the  $5/2^+$ [622] state. Values of the same order of magnitude had been obtained in  $^{247}\text{Cm}$  (7.3(21) W.u) and  $^{249}\text{Cf}$  (10(4) W.u), indicating the presence of strong octupole correlations. As pointed out earlier, octupole correlations arise due to the presence at the Fermi level of neutron orbitals stemming from the  $g_{9/2}$  and  $j_{15/2}$  neutron shells. There are also proton orbitals with similar  $\Delta j = \Delta l = 3$  characteristics; the  $7/2^+$ [633] and  $3/2^-$ [521] orbitals originating from the proton  $i_{13/2}$  shells and  $f_{7/2}$ . Excitations involving these orbital lead to a low-lying  $2^-$  octupole phonon, which lies at a record excitation energy of 593 keV in  $^{248}\text{Cf}$  [12]. The interaction between phonon and quasiparticle excitations is therefore an important ingredient to properly describe excited states in this region.

The last known N=151 isotone is  $^{255}\text{Rf}$ . Its low-lying structure had been previously investigated by  $\alpha$  spectroscopy of  $^{259}\text{Sg}$  at GSI [32]. The experiment had established the presence of 2  $\alpha$ -emitting states and suggested a change in the structure of the ground state as compared to systematics of N=153 isotones due to an inversion between the  $1/2^+$ [620] and the  $11/2^-$ [725] states, the latter becoming the ground state in  $^{259}\text{Sg}$  and the former becoming an isomeric state at  $\sim 90$  keV above the ground state. The experiment also revealed a delayed low-energy signal in the implantation detector following the  $\alpha$  decay of the 90 keV isomer, most likely due to the  $5/2^+ \rightarrow 9/2^-$  M2 transition in  $^{255}\text{Rf}$ . The half-life of the decaying state was measured to be 50(17)  $\mu\text{s}$ . No K X rays were detected in coincidence and the excitation energy was estimated to be  $\sim 135$  keV.  $^{255}\text{Rf}$  was reinvestigated recently in direct production at SHIP and also SHELS. Two higher-lying isomers were observed in both cases [21,33]. The contribution of the M2 decay of the  $5/2^+$ [622] state to the total isomeric signal observed in the implantation detector and the tunnel detectors could be extracted from the GABRIELA data using a GEANT4-assisted analysis, establishing the excitation energy of the  $5/2^+$ [622] state in  $^{255}\text{Rf}$  to be 150 keV [21].

As already mentioned before and shown in the next section, the fact that

the  $11/2^- [725]$  state is suggested to be a very low-lying  $\alpha$ -emitting isomer in  $^{257}\text{Rf}$  [29, 34–37] and the ground state in  $^{259}\text{Sg}$  [32] means fine structure  $\alpha$ -decay studies may reveal the whereabouts of the  $11/2^-$  state in the daughter nuclei. Antalic et al. [32] observed an unhindered  $\alpha$  branch from the ground state of  $^{259}\text{Sg}$  to a state at  $\sim 600$  keV above the ground state in  $^{255}\text{Rf}$ . This state was tentatively assigned to be based on the  $11/2^- [725]$  Nilsson state. A recent study of the  $\alpha$  decay of  $^{257}\text{Rf}$  using GABRIELA has demonstrated that an unhindered  $\alpha$  decay branch of the low-lying isomeric state of  $^{257}\text{Rf}$  populates a state at 750 keV above the  $9/2^- [734]$  ground state and that the 750 keV transition to the ground state is a magnetic dipole transition [38]. This establishes the spin and parity of the state in  $^{253}\text{No}$  and the isomer in  $^{257}\text{Rf}$  to be  $11/2^-$ .

### 3.1.3 $N=153$ isotones

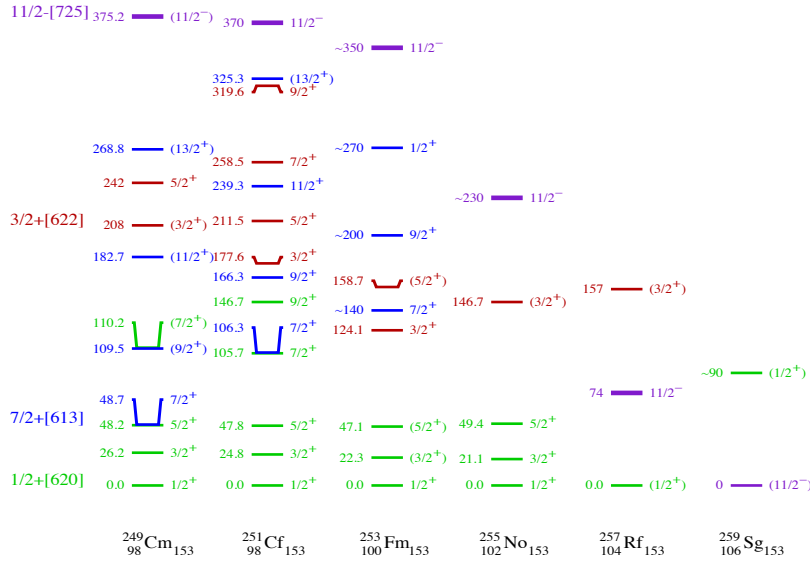


**Fig. 8** Systematics of the lowest states in  $N=153$  isotones. The excitation energy of the  $11/2^- [725]$  state is rather constant in  $^{249}\text{Cm}$  and  $^{251}\text{Cf}$ , but from  $^{253}\text{Fm}$  onwards it steadily decreases to become the suggested ground state of  $^{259}\text{Sg}$ . The half-life of the state increases accordingly, taking on values of 19(1) ns, 1.3(1)  $\mu\text{s}$ , 0.56(6)  $\mu\text{s}$ ,  $\sim 100$   $\mu\text{s}$ , 4.5(1) s and 402(56) ms in  $^{249}\text{Cm}$ ,  $^{251}\text{Cf}$ ,  $^{253}\text{Fm}$ ,  $^{255}\text{No}$ ,  $^{257}\text{Rf}$  and  $^{259}\text{Sg}$  respectively. The data is taken from Refs. [11, 39, 40, 36].

Until recently, very little spectroscopic information on  $^{255}\text{No}$  was available. Using the reactions  $^{238}\text{U}(^{22}\text{Ne}, 5n)^{255}\text{No}$  and  $^{208}\text{Pb}(^{48}\text{Ca}, 1n)^{255}\text{No}$ , two experiments performed with GABRIELA have revealed the presence of four isomeric decays in cascade followed by the characteristic  $\alpha$  decay of  $^{255}\text{No}$  and

the M2 isomeric decay from the  $5/2^+[622]$  state in the daughter nucleus  $^{251}\text{Fm}$  [39]. The lowest-energy isomeric state has a half-life of  $\sim 100 \mu\text{s}$  and lies at an excitation energy of  $\sim 230 \text{ keV}$  above the ground state. Strong L X rays are observed in coincidence with this isomeric decay and also a weak  $118 \text{ keV}$   $\gamma$ -ray line. Given the decoupling parameter of the  $1/2^+[620]$  ground state configuration extracted from the ground state rotational sequence in lighter  $N=153$  isotones, the  $9/2^+$  member of the ground state band is expected to lie below  $150 \text{ keV}$  excitation energy. From the systematics of Fig. 8, one also expects the presence of the  $3/2^+[622]$  at low excitation energy. In terms of isomeric configuration, a likely assignment for the isomer is the  $11/2^- [725]$  Nilsson state, whose excitation energy is seen to steadily decrease in  $N=153$  isotones and become the ground state in  $^{259}\text{Sg}$ . If the  $11/2^- [725]$  state were to decay to the  $9/2^+$  member of the ground state band, the  $\gamma$ -ray spectrum would be dominated by a  $80\text{-}100 \text{ keV}$  E1 line, which is not the case. The data seems to indicate that the decay proceeds through an intermediate band before reaching the ground state and that the observed weak line at  $118 \text{ keV}$  must be an E2 transition, possibly the  $9/2^+ \rightarrow 5/2^+$  transition in the  $3/2^+[622]$  band. Given the total calorimetric energy measured in the isomeric decay and the lack of any, this in turn would put the  $3/2^+$  band head at  $\sim 50 \text{ keV}$  above the ground state, continuing the trend of decreasing excitation energy observed from  $^{249}\text{Cm}$  to  $^{253}\text{Fm}$  in Fig. 8. This is however at odds with unpublished data from JAEA [40], where  $\gamma$  rays following the decay of  $^{259}\text{Rf}$  have been observed and assigned to the decay of the  $3/2^+[622]$  state by analogy to the decay of the lighter isotone  $^{257}\text{No}$  [41] (the same analogy was also used to assign the decay of the  $3/2^+[622]$  state in  $^{257}\text{Rf}$  [36]). This assignment places the  $3/2^+[622]$  at a higher excitation energy of  $147 \text{ keV}$  (as shown in Fig. 8). More spectroscopic data for the  $N=153$  and  $155$  isotones is clearly needed to understand the sequence of low-lying states and resolve this discrepancy.

### 3.2 $K$ isomers

In axially deformed nuclei, the  $K$  quantum number is approximately conserved. Transitions that involve a change in  $K$  larger than the multipole order  $\lambda$  are usually forbidden and  $K$  isomers are formed. The combination of deformation and coexistence of high and low- $j$  orbitals at the Fermi surface leads to high- $K$  isomers in the  $^{254}\text{No}$  region (see [42] for a recent review). The properties of  $K$  isomers provide a unique fingerprint of the underlying single-particle structure. They also provide an experimental tool to access low-lying states that are not readily populated by  $\alpha$  decay or difficult to observe at the target in prompt spectroscopy experiments either due to internal conversion or weak population. Multi-quasiparticle states such as high- $K$  states are also predicted to be more stable against fission than the ground state and populating these states should lead to an enhanced survival probability of super heavy nuclei [43, 44].

The early campaigns with GABRIELA were limited with regards to high- $K$

isomer searches as the thresholds in the implantation detector did not allow to detect the low energy signals induced by the typical isomeric cascade of ICEs and accompanying atomic emissions (see [45] for more details). Two new isomers were nevertheless identified in  $^{253}\text{No}$  [28] and  $^{255}\text{Lr}$  [46] through the observation of isomeric decays of up to a few ms in the tunnel detectors. With the upgraded version of GABRIELA, new isomers have also been found in  $^{255,256}\text{No}$  [39,47] and new data has been collected to study the electromagnetic decay of known high- $K$  isomers, and in particular, to determine their fission branch. In the next sections, a non exhaustive selection of results will be presented and discussed.

### 3.2.1 $^{253}\text{No}$

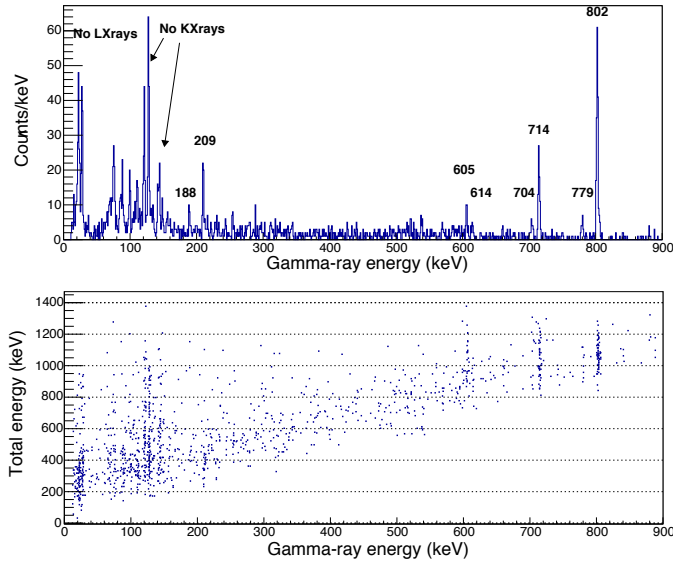


**Fig. 9** Top) Spectrum of  $\gamma$  rays coincident with a low-energy DSSD signal registered within 8 ms of the implantation of a heavy nucleus produced in  $^{48}\text{Ca}$ -induced reactions on a  $^{207}\text{Pb}$  target. Bottom) Sum of the energies of the isomeric signals detected in all the Si and Ge detectors of GABRIELA vs coincident  $\gamma$  rays with the added requirement that the characteristic  $\alpha$  decay of  $^{253}\text{No}$  be subsequently detected in the DSSD.

While studying the decay properties of the low-lying  $5/2^+[622]$  state in  $^{253}\text{No}$ , the presence of a longer-lived high- $K$  state was evidenced in the time distribution of ICEs detected in the tunnel detectors of GABRIELA following the implantation of ERs produced in the reaction  $^{207}\text{Pb}(^{48}\text{Ca}, \text{xn})^{255-x}\text{No}$ . No spectroscopic information could be extracted due to the underlying contribution of randomly-correlated ICEs, but the half-life of the isomer was measured to be  $970(200) \mu\text{s}$ . The existence of this long-lived isomeric state was subse-

quently confirmed by GSI data [48,49]. In the last experiment performed with GABRIELA coupled to the VASSILISSA separator in 2009 [50], this time using Jones's isomer-decay tagging method [6], the spectrum of  $\gamma$  rays emitted in the isomer decay could be extracted (see top panel of Fig. 9). The decay involves high-energy  $\gamma$  rays (802 and 714 keV for instance), which had previously been observed at the target position in a prompt spectroscopy experiment [51]. This means that the decay proceeds by at least one intermediate structure that decays promptly to the ground state band. An estimate of the excitation energy of the isomer can be made from the bottom panel of Fig. 9, which shows that the maximum energy detected in the decay is around 1.2-1.3 MeV. Despite the statistics accumulated at both GSI and Dubna, no complete decay scheme has so far been established for this isomer, whose structure remains therefore uncertain.

### 3.2.2 $^{255}\text{Lr}$

In  $^{255}\text{Lr}$ , the search for isomeric ICEs in the tunnel detectors of GABRIELA revealed the existence of a 1.4(1) ms isomer. Based on coincidences between these ICEs and  $\gamma$  rays, a lower limit of 720 keV could be established for the excitation energy of the isomer, which was subsequently also observed at GSI and Berkeley [52,53]. In these experiments, the isomeric decay was observed by detecting the cascade of conversion electrons and coincident atomic radiation at the same position as the implanted recoil in the focal plane Si-strip detector. From the spectrum of coincident  $\gamma$  rays, Jeppesen et al. [53], established a decay scheme and assigned the isomeric state to a structure based on two quasineutrons coupled to the odd proton, which decays via two intermediate structures to a band built on the  $i_{13/2}$   $9/2^+$  [624] proton configuration of Fig. 10. In the published scheme, two transitions of 244 and 301 keV depopulate the isomer and three transitions of 387, 494 and 588 keV connect the lowest intermediate band head to members of the  $9/2^+$  [624] band. No decay out of the  $9/2^+$  [624] band head was observed and the authors deduced that the excitation energy of the  $9/2^+$  [624] state with respect to the  $7/2^-$  [514] isomer in  $^{255}\text{Lr}$  must be less than 30 keV. Given the  $\sim 30$  keV excitation energy of the  $7/2^-$  [514] isomeric state extracted from recent mass measurements at SHIPTRAP [54], the decay scheme established by Jeppesen et al. [53] entails an excitation energy of the lowest intermediate ( $15/2^+$ ) state of at most 800 keV, which is  $\sim 200$  keV lower than the  $3^+$  state in  $^{254}\text{No}$  [55,56,2,57] and  $\sim 100$  keV lower than the  $2^-$  octupole-phonon state in  $^{250}\text{Fm}$  and  $^{252}\text{No}$  [58,59]. This is a remarkably low excitation energy for a three quasiparticle state.

The other issue with the proposed decay scheme, namely the small energy separation between the  $9/2^+$  [624] state and the  $7/2^-$  [514] states in  $^{255}\text{Lr}$ , finds its roots in the interpretation of the  $8^-$  isomer of  $^{254}\text{No}$  [55,56,2,57]. Fig. 10 shows the relevant single-particle orbitals available around the Fermi surface for  $^{254}\text{No}$ . If indeed the proton  $9/2^+$  [624] configuration favourably-coupled with the proton  $7/2^-$  [514] configuration is involved in the  $8^-$  isomeric state, the fact that the excitation energy of the isomer is 1.297(2) MeV together



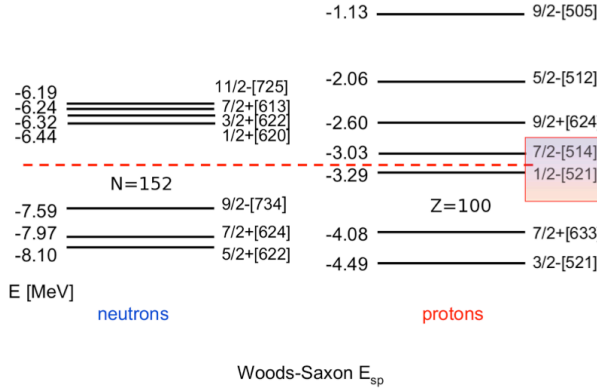


**Fig. 10** Single-particle neutron and proton levels obtained with the Universal Woods-Saxon potential [60]. The dashed line represents the Fermi surface in  $^{254}\text{No}$ . At the Fermi surface the  $7/2^- [514]$  and  $1/2^- [521]$  orbitals are almost degenerate and experimental evidence has established a reversed ordering of the  $1/2^-$  and  $7/2^-$  states at the deformation relevant for  $^{255}\text{Lr}$  [61, 62].

with the observed proximity of the  $7/2^- [514]$  and  $1/2^- [521]$  states in  $^{255}\text{Lr}$  and  $^{251}\text{Md}$  [54, 61, 62] would imply that the energy separation between the  $9/2^+ [624]$  and  $7/2^- [514]$  states should be quite large, which is at odds with the conclusions of Jeppesen et al. [53]. The nature of the  $8^-$  state is still under debate and only a measurement of the splitting of its hyperfine structure can determine unambiguously whether the state is based on a two-quasiproton excitation or whether it involves a two-quasi-neutron excitation, or a mixture of both. This is because, although the intrinsic  $g_K$  factors of the possible two-quasiparticle states are very different ( $g_K \approx 1$  for the two-proton excitation involving the  $7/2^+ [514]$  and  $9/2^+ [624]$  single-particle states and  $g_K \approx -0.28$  for the two-neutron excitation involving the  $7/2^+ [613]$  and  $9/2^- [734]$  states), the electromagnetic properties of the intra-band decays should be quite similar, given the absolute value of  $|g_K - g_R|$ , where  $g_R$  is the rotational  $g$  factor ( $0.7Z/A \leq g_R \leq Z/A$ ). Pinning down the excitation energy of the  $9/2^+ [624]$  state in  $^{255}\text{Lr}$ , either by prompt or decay spectroscopy, would give valuable information on the structure of odd- $Z$  nuclei above  $Z=100$ , as this state has only been tentatively identified in  $^{257}\text{Db}$  and  $^{253}\text{Lr}$  [63],  $^{247,249}\text{Bk}$  [64, 65] and  $^{251}\text{Es}$  [66].

### 3.2.3 Fission hindrance

In a review of hindered decays of  $K$  isomers [42], the hindrance factor defined as  $HF = T_{1/2, \text{isomer}}^{SF} / T_{1/2, \text{ground state}}^{SF}$  was deduced for the isomers with a reported spontaneous-fission branch. Except for  $^{250}\text{No}$ , the available experimental evidence did not seem to indicate a higher hindrance for spontaneous fission from  $K$  isomers, which is at odds with estimates of expected fission

hindrances due to the specialisation energy and reduced pairing fields associated with high- $K$  states [67]. Since the publication of the review, two isomers in  $^{254}\text{Rf}$  [68] were observed to have a longer partial fission half-life than the ground state.

In order to understand the fission from high- $K$  isomeric states, the available data needs to be verified with higher experimental sensitivity. This is the reason why dedicated experiments were performed with GABRIELA at SHELS to remeasure or measure for the first time the fission branch from the known low-lying isomers in  $^{250,252,254}\text{No}$ . In both  $^{250}\text{No}$  and  $^{254}\text{No}$ , the fission hindrances are found to be larger than previously established. These results will be the object of a forthcoming publication [69].

## 4 Perspectives

### 4.1 Clover array

The Ge-detector array of GABRIELA will soon be upgraded to a 5 Compton-Suppressed Clover Ge array. This will increase the detection efficiency and granularity required to disentangle multiple-photon cascades, such as those accompanying the decay of high- $K$  isomers. GEANT4 simulations have guided the design of a new detector chamber for the new clover array. Special high density tungsten shields have also been designed in order to reduce drastically the background and cross talk for the  $\gamma$ -ray detectors. Such a Densimet liner inside the chamber should reduce the background count rate induced by the 1461 keV line from  $^{40}\text{K}$  by a factor of almost 5.

### 4.2 Front-End and Back-End Electronics

A fully digital data acquisition system using state of the art digitizers from National Instruments is under development for GABRIELA. While having an excellent energy resolution for Si detectors (14-16 keV FWHM at 5499 keV and a full-scale of  $\sim 250$  MeV) GABRIELA's current preamplifiers from TechInvest do not have a fast enough rise-time to achieve ns timing when coupled to the new digital electronics. Not only are faster rise-times required for better timing, but they are also needed to construct a faster trigger in order separate events that would otherwise have been considered pile-up. The design and tests of preamplifiers based on those from the SIRIUS collaboration [70] is currently on going. Resolutions of  $\sim 8$  keV FWHM at 320 keV and  $\sim 14$  keV at 5805 keV with an effective full-scale range of  $\sim 180$  MeV and a threshold of  $\sim 75$  keV have been measured. Having a low-energy threshold in the implantation DSSD is extremely important for Jones' isomer-decay tagging technique [6] as it allows the  $\gamma$  rays and ICEs, measured in the germanium and tunnel detectors, that are emitted in coincidence with the signal in the DSSD to be pulled out of the background. The importance of having the lowest possible threshold is

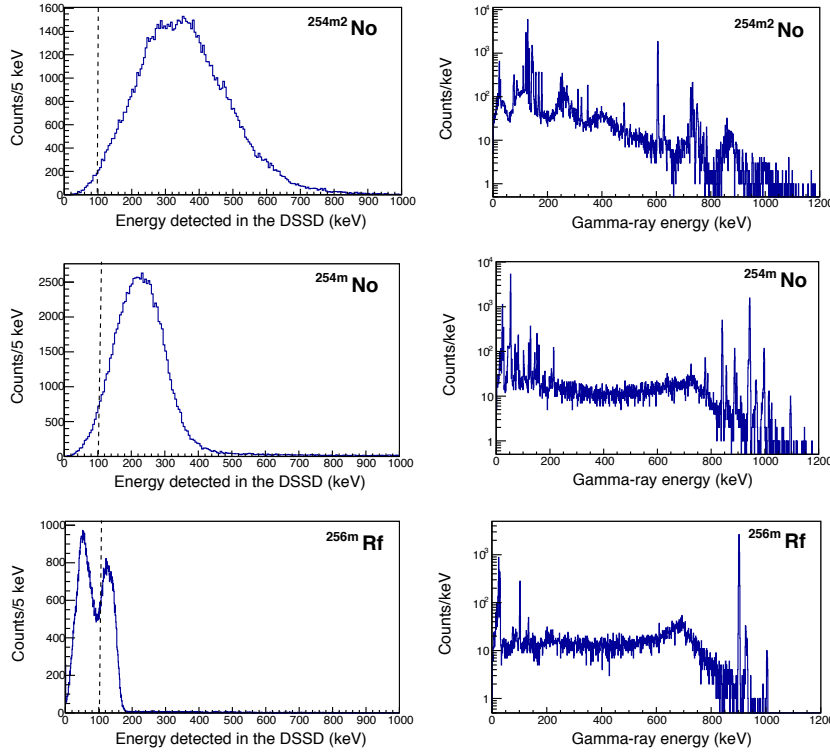


**Fig. 11** From top to bottom) Simulated energy depositions in the DSSD (left panels) and in the Ge array of GABRIELA (right panels) in the decay of the 265 ms isomer in  $^{254}\text{No}$ , the 184  $\mu\text{s}$  isomer in  $^{254}\text{No}$  and the lowest high- $K$  isomer in  $^{256}\text{Rf}$  (see text for details).

illustrated in Fig. 11 where the energy deposited in the implantation detector following the decay of different isomers has been simulated in GEANT4 [9]. The published decay scheme of Ref. [2] was taken as input to generate the primary emissions from the long-lived  $^{254m}\text{No}$  and short-lived  $^{254m2}\text{No}$  isomers. For the decay of the lowest-lying isomer in  $^{256}\text{Rf}$  [71,72], the isomer is assumed to decay directly to the  $4^+$  member of the ground state rotational band via the emission of a 900 keV transition. Such a decay scenario is corroborated by unpublished data taken with GABRIELA and also by the fact that the 900 keV transition observed by Jeppesen et al., [71] was not observed at the target position [73,74] and cannot therefore correspond to the decay of an intermediate structure, as suggested in [71]. Fig. 11 clearly shows that with a threshold of 100 keV, less than half of the decays from the lowest isomer in  $^{256}\text{Rf}$  would trigger the acquisition. It also illustrates that isomeric ratios extracted from the observed signals in the DSSD are not a meaningful quantity to determine the underlying nature of multi-quasiparticle states, as the number of detected isomeric signals in the DSSD depends on the decay scheme of the isomer, which is unfortunately often poorly known or not known at all.

## 5 Summary

Over the years, the GABRIELA collaboration has built a state-of-the-art setup for spectroscopic studies of transfermium nuclei and has developed new analysis techniques to extract as much physical information as possible from the data. The most recent campaigns have provided a wealth of new data that is still being analysed. Combined  $\alpha$  and/or  $\gamma$  and ICE spectroscopy has allowed to extend our knowledge on the properties and sequence of nuclear states in  $N=148$ -154 isotones. Another topic of interest has been the fission properties of high- $K$  isomers. Here we have improved the existing data for No isotopes. Such investigations require long irradiation times in order to be able to evidence the presence (or lack of) of weak fission branches and will no doubt benefit from the increased beam intensities available at the upcoming facilities worldwide. They also pose a theoretical challenge as how to properly model the fission of a high- $K$  state is still an open question. The ongoing upgrade to GABRIELA, with a better efficiency, signal-to-noise ratio and improved dynamic range and timing resolution, should allow to push investigations to heavier and fast-decaying nuclei as well as revisit some physics cases. In the future, GABRIELA will also be used at the focal plane of the third Dubna Gas-filled Recoil Separator recently installed at the Super Heavy Element Factory and which should soon be commissioned.

**Acknowledgements** The GABRIELA project is jointly funded by JINR (Russia) and IN2P3/CNRS (France). Financial support from the Russian Foundation for Basic Research, the French National Research Agency ANR, the JINR-BMBF (Germany), JINR-Polish, and JINR-Slovak Cooperation Programmes as well as from the Norwegian Research Council and the Bulgarian National Science Fund is also acknowledged.

## References

1. Ch. Theisen et al., Nucl. Phys. A 944 (2015) 333
2. R.M. Clark, Phys. Lett. B690 (2010) 19-24
3. A. Yeremin et al., Nucl. Instr. Meth. A 350 (1994) 608
4. K. Hauschild et al., Nucl. Instr. Meth. A 560 (2006) 388
5. A. Isaev et al., Instruments and Experimental Techniques 54 (2011) 37
6. G.D. Jones, Nucl. Instr. Meth. A 488 (2002) 471
7. A. Popeko et al., Nucl. Instr. Meth. B 376 (2016) 140
8. R. Chakma et al., Eur. Phys. J. A 56 (2020) 245
9. S. Agostinelli et al., Nucl. Instrum. Methods A506 (2003) 250
10. A. Lopez-Martens et al., Phys. Rev. C 74 (2006) 044303
11. Evaluated Nuclear Structure Data File (ENSDF)
12. S. Yates et al., Phys. Rev. C 12 (1975) 442
13. N.Yu. Shirikova et al., Phys. Rev. C 88 (2013) 064319
14. N.Yu. Shirikova et al., Eur. Phys. J. A 51 (2015) 21
15. S. Raeder et al., Phys. Rev. Lett. 120 (2018) 232503
16. F.P. Hessberger et al., Eur. Phys. J. A 48 (2012) 75
17. T. Kibédi, T.W. Burrows, M.B. Trzhaskovskaya, P.M. Davidson, C.W. Nestor Jr., Nucl. Instr. and Meth. A 589 (2008) 202-229
18. R.R. Chasman et al., Rev. Mod. Phys. 49 (1977) 833
19. I. Ahmad, Phys. Rev. C 8 (1973) 737

20. F.P. Hessberger et al., Eur. Phys. J. A 29 (2006) 165
21. R. Chakma, PhD, Université Paris Saclay (2020)
22. J. Khuyagbaatar et al., Phys. Rev. C 104, L031303 (2021).
23. A. Lopez-Martens et al., Phys. Rev. C 105 (2022) L021306
24. A. I. Svirikhin et al., Phys. of Part. and Nucl. Lett. 18, 445 (2021).
25. M.S. Tezekbayeva et al., Eur. Phys. J. A 58 (2022) 52
26. A. Sobiczewski and K. Pomorski, Prog. in Part. and Nucl. Phys. 58 (2007) 292
27. E. Bemis et al., Phys. Rev. Lett. 31 (1973) 647
28. A. Lopez-Martens et al., Eur. Phys. J. A 32 (2007) 245
29. F.P. Hessberger et al., , Z. Phys. A 359 (1997) 415
30. K. Rezyunkina et al., Nucl. Instr. Meth. A 844 (2017) 96
31. K. Rezyunkina et al., Phys. Rev. C 97 (2018) 054332
32. S. Antalic et al., Eur. Phys. J. A 51 (2015) 41
33. P. Mosat et al., Phys. Rev. C 101 (2020) 034310
34. J. Qian et al., Phys. Rev. C 79 (2009) 064319
35. J. S. Berryman et al., Phys. Rev. C 81 (2010) 064325
36. B. Streicher et al., Eur. Phys. J. A 45 (2010) 275
37. J. Rissanen et al., Phys. Rev. C 88 (2013) 044313
38. K. Hauschild et al., Eur. Phys. J. A 58 (2022) 6
39. K. Kessaci et al., PhD, Université de Strasbourg (2022)
40. M. Asai et al., JAEA-Tokai tandem annual report 2008
41. M. Asai et al., Phys. Rev. Lett. 95 (2005) 102502
42. F. Kondev, G. Dracoulis and T. Kibédi, Atomic Data and Nuclear Data Tables 103-104 (2015) 50
43. F. Xu et al. Phys. Rev. Lett. 92 (2004) 252401
44. P. Jachimowicz, M. Kowal, and J. Skalski Phys. Rev. C 92(2015) 044306
45. Ch. Theisen, A. Lopez-Martens and Ch. Bonnelle, Nucl. Instr. Meth. A 589 (2008) 230
46. K. Hauschild et al., Phys. Rev. C 78 (2008) 021302(R)
47. K. Kessaci et al., Phys. Rev. C 104 (2021) 044609
48. S. Antalic et al., Eur. Phys. J. A (2011) 47
49. F.P. Hessberger et al., Physics of Atomic Nuclei 70 (2007) 1445
50. A. Lopez-Martens et al., Nucl. Phys. A 852 (2011) 15
51. S. Eeckhaudt, PhD Thesis, University of Jyväskylä (2006)
52. S. Antalic et al., Eur. Phys. J. A 38 (2008) 219
53. H.B. Jeppesen et al., Phys. Rev. C 80 (2009) 034324
54. F. Giacoppo et al., in preparation
55. S.K. Tandel et al., Phys. Rev. Lett. 97 (2006) 082502
56. R.-D. Herzberg et al., Nature 442 (2006) 896
57. F.P. Hessberger et al., Eur. Phys. J. A 43 (2010) 55
58. P.T. Greenlees et al., Phys. Rev. C 78 (2008) 021303(R)
59. B. Sulignano et al., Eur. Phys. J. A 33 (2007) 327
60. S. Ćwiok, J. Dudek, W. Nazarewicz, J. Skalski, and T. Werner, Comput. Phys. Commun. 46, 379 (1987)
61. A. Chatillon et al., Eur. Phys. J. 30 (2006) 397
62. M. Asai, F. Hessberger and A. Lopez-Martens, Nucl. Phys. A 944 (2015) 308
63. F.P. Hessberger et al., Eur. Phys. J. A 12 (2001) 57
64. I. Ahmad, Phys. Rev. C 20 (1979) 290
65. I. Ahmad Phys. Rev. C 71 (2005) 054305
66. I. Ahmad Phys. Rev. C 17 (1978) 2163
67. R.M. Clark, EPJ Web of Conferences 131 (2016) 02002
68. H. David et al., Phys. Rev. Lett. 115 (2015) 132502
69. A. Lopez-Martens et al., to be published
70. F. Dechery et al., Nucl. Instr. Meth. B 376 (2016) 125
71. H.B. Jeppesen et al., Phys. Rev. C 79 (2009) 031303(R)
72. A. Robinson et al., Phys. Rev. C 83 (2011) 064311
73. P.T. Greenlees et al., Phys. Rev. Lett. 109 (2012) 012501
74. J. Rubert, PhD Université de Strasbourg (2013)